

CONFIGURATION DESIGN AND 3D-FEM ANALYSIS FOR A RADIAL-AXIAL HYBRID MAGNETIC BEARING

Qinghai Wu

School of Electrical and Information Engineering, Jiangsu University, Zhenjiang 212013, China
wqh29902345@163.com

Huangqiu Zhu, Dehong Zhu, Yuxiang Shen

School of Electrical and Information Engineering, Jiangsu University, Zhenjiang 212013, China
zhuhuangqiu@ujs.edu.cn

ABSTRACT

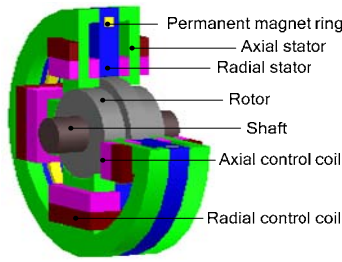
In this paper, an innovated radial-axial hybrid magnetic bearing (HMB) is proposed, which is driven by a 2-phase AC power inverter in radial directions and a DC amplifier in axial direction respectively. The axial and radial biased magnetic fluxes of this magnetic bearing are provided by a common radial polarized permanent magnet ring, and the axial and radial control magnetic fluxes are provided by the inner and outer two-layer coils, respectively. The configuration and the principle producing magnetic suspension forces of the radial-axial HMB are introduced. The flux path is calculated by using the method of equivalent magnetic circuit, the mathematics models of the axial and radial magnetic suspension forces are deduced. The experiment prototype of the innovated bearing is designed and the practical prototype's parameters are given. The feasibility and the correctness of the theoretical methods for the configuration, magnetic path and maximum loads capacity of the radial-axial HMB are verified by using a 3D-FEM software (Maxwell 3D of ANSOFT). The theoretical approach and finite element simulated experiment have shown that the mechanical structure and magnetic circuit of this magnetic bearing are legitimacy. The radial control flux and the axial control flux are independent, the magnetic paths between radial direction and axial direction have no coupling. This radial-axial HMB can be applied in high speed machine tool spindle with lower manufacturing and operation costs.

INTRODUCTION

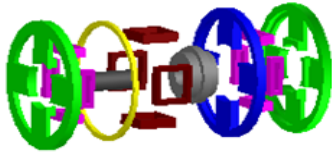
Magnetic bearing is a kind of high technology electromechanical products, which has realized no machinery friction between the rotor and the stator.

Magnetic bearings can be classified as DC magnetic bearing and AC magnetic bearing by its exciting current types. A radial magnetic bearing is usually operated by two channel bipolar power amplifiers (or four channel unipolar power amplifiers) at least, and the cost of DC power amplifier is high, the weight and losses are bigger. However, an AC magnetic bearing can be driven by an industrial AC power inverter. 2 degrees of freedom in radial direction can be controlled by an AC power inverter completely. Moreover, AC power inverters are used in huge quantities for electrical drives and are available at very low price^[1], they can be incorporated with high performance DSP, which makes it very easy to rewrite or update the software of the controller in a magnetic bearing system.

Any stable revolution rotor system needs to be controlled in 5 degrees of freedom, so it is usually composed of an axial degree of freedom AMB and 2 radial 2 degrees of freedom AMB. This kind of configurable magnetism magnetic bearing system has a large axial size. Moreover, DC power amplifiers have many disadvantages, such as large volume, high power losses and high price that limit the reality applies of AMBs in high-speed flywheels, super-speed and super-precision numerical control machine tools, satellites, etc.. Therefore, a radial-axial magnetic bearing combines an axial degree of freedom magnetic bearing and a radial 2 degrees of freedom magnetic bearing into a whole one becomes one of magnetic bearing research direction. At present, DC radial-axial HMBs have been designed^[2], AC radial 2 degrees of freedom HMBs have been designed too and applied in the bearingless canned motor pump in Switzerland^[3]. Our research team has developed a kind of 3-pole AC-DC 3 degrees freedom HMB^[4,5]. On this basis, this innovated radial-axial HMB has been designed, which is driven and controlled by a



(a) Assembling structure of the radial-axial HMB



(b) Exploded view of radial-axial HMB components

FIGURE 1: Configuration of the proposed radial-axial HMB

2-phase AC power inverter in radial directions and DC amplifier in axial direction. It has a potential application in super-speed and super-precision numerical control machine tools, magnetic suspension bearingless motors, high-speed flywheels, satellites, and so on.

CONFIGURATION AND OPERATING PRINCIPLE

Configuration of Radial-axial HMB

Figure 1 shows the configuration of the proposed radial-axial HMB, which consists of two slices axial stator with radial-axial bilateral magnetic pole face structure, eight axial control coils, a radial stator with four poles, four radial control coils, a permanent magnet ring magnetized radially, a rotor and a shaft, etc..

The axial and radial biased magnetic fluxes of this kind of magnetic bearing are provided by a common permanent magnet ring magnetized radially, and the permanent magnet material is neodymium-iron-boron. The permanent magnet ring is split into four pieces as it is easy to processing and being implanted into the radial stator. Then the four pieces of permanent magnet are jointed into an overall permanent magnet ring. There are two slices axial stator with radial-axial bilateral magnetic pole face structure, and every slice is composed of 4 radial-axial bilateral magnetic pole face iron cores arranged around the rotor symmetrically. The 4 poles of the radial stator are arranged around the rotor symmetrically, and every radial pole is arranged between 2 axial relative axial poles. Both the radial stator and the axial stator are made of annular silicon steel sheets. The rotor is made of annular silicon steel

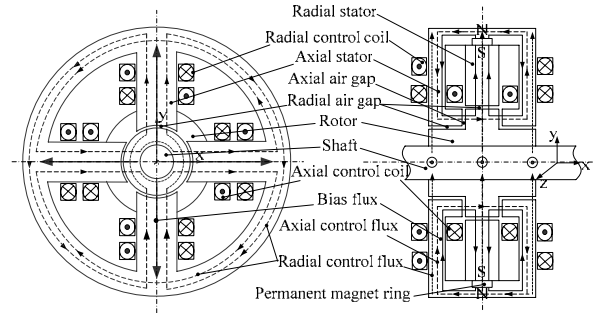


FIGURE 2: Magnetic flux path of radial-axial HMB

sheets, too. The axial and radial control magnetic fluxes are provided by the inner and outer two-layer coils, respectively. The flux generated by all of the axial control coils is used to control the axial single degree of freedom, and the resultant flux generated by four radial coils arranged around the rotor is used to control the radial 2 degrees of freedom. If there is no external disturbance or load, the static attracting forces generated by the permanent magnet will levitate the rotor in the ideal balance position.

Operating Principle of Radial-Axial HMB

The magnetic flux path of the radial-axial HMB is presented in figure 2. The real lines with arrows represent the static biased flux generated by the permanent magnet ring, which start from N-pole of the permanent magnet ring, flow through the axial stator, the axial air gap, the rotor, the radial air gap, then come back through the radial stator to S-pole of the permanent magnet ring. The dashed lines with arrows (the arrow direction of the control magnetic flux is determined by the control current direction in right hand rule) represent the control fluxes generated by the control coils. The radial control flux is conducted by the radial stator, radial air gap and the rotor, and the axial control flux is conducted by the axial stator, axial air gap and the rotor. As shown in figure 2, the axial flux and the radial flux do not influence each other, so there is no coupling between them. The static biased flux and the control flux are superimposed or subtracted in each air gap.

The flux quantities of permanent biased magnetic fluxes are the same in both of the axial air gaps when the rotor is in the axial reference balance position. If the rotor is displaced in the axial direction by a disturbance force, the axial permanent flux ϕ_{pz1} will be increased and the magnetic force will be increased correspondingly in the reduced air gap. Whereas the other axial permanent flux ϕ_{pz2} will be reduced in the increased air gap, the magnetic force will be decreased. As long as the control flux ϕ_{cz} contents the following expression:

$$\phi_{cz} \geq \frac{\phi_{pz1} - \phi_{pz2}}{2} \quad (1)$$

Then no matter a left or right external disturbance is applied to the rotor, the axial control system with a negative position feedback will adjust the exciting current of the axial control coils to control the flux of the air gap, and levitate the rotor in the ideal axial balance position.

The radial operating principle of the radial-axial HMB is based on principle of bearingless motor. Superposing an additional bearing windings flux distribution with pole pair number $p_2 = p_1 \pm 1$ ^[6], p_1 is the pole pair number of motor windings. Maxwell lateral forces can be set up and be used to support the rotor without contact. If $p_1=0$, $p_2=1$, the bearingless motor is changed to be a radial magnetic bearing with radial suspension force in fact. Based on motor theories, 2 radial coils differ by 90° in space imported 2-phase balanced AC differ by 90° on time, and the same to the other 2 radial coils, the exciting current would generate a rotated magnetic field and form a unipolar incorporated magnetic flux. When the rotor is displaced from the balance position due to radial disturbances, the radial position sensors measure the position of the rotor and transfer the position signals to the controller. The controller calculates the displacements x and y , and transforms them into control current signals. The power amplifier is driven by the control signals and outputs exciting currents, in this way, the exciting currents generate control flux, which is superposed with the biased flux. So adjusting exciting currents, the resulting force generated by the biased and the controllable fluxes can be pointed in any direction and levitate the rotor in the ideal radial position.

MATHEMATICS MODELS

Calculation of the Equivalent Magnetic Flux Path

To simplify calculation of the magnetic flux path, there are some assumptions on the flux path. Only the leakage of the inner and outer annulus of the permanent magnet are considered, the whole flux path system is taken as a parallel connection system composed by leakage reluctance and available fluxes. And as well, only the air gap reluctance is considered, the reluctance of the stator core and the rotor, the hysteresis and the eddy current losses of the radial-axial HMB are neglected. Therefore, the equivalent permanent magnet circuit is laid out in figure 3.

In figure 3, F_m is the magnetic motive force (MMF) that the permanent magnet provides to the outer circuit, ϕ_m is the total magnetic flux that the permanent magnet generates, ϕ_s is the total magnetic flux leakage of the permanent magnet, the leakage permeance is G_s , G_{z1} and

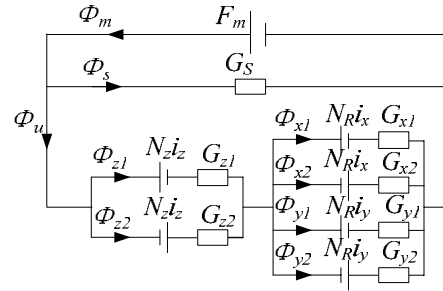


FIGURE 3: Equivalent flux path of radial- axial HMB

G_{z2} describe the positive and the negative air gap permeance respectively, the radial air gap permeances are G_{x1} , G_{x2} , G_{y1} and G_{y2} respectively. Supposing that the rotor has a positive displacement z in the axial direction, and has positive displacements x and y in the two directions x and y respectively, then the magnetic permeance of each air gap can be calculated as follows:

$$\begin{cases} G_{z1} = \frac{\mu_0 S_z}{\delta_z - z} & G_{z2} = \frac{\mu_0 S_z}{\delta_z + z} \\ G_{x1} = \frac{\mu_0 S_R}{\delta_R - x} & G_{x2} = \frac{\mu_0 S_R}{\delta_R + x} \\ G_{y1} = \frac{\mu_0 S_R}{\delta_R - y} & G_{y2} = \frac{\mu_0 S_R}{\delta_R + y} \end{cases} \quad (2)$$

where μ_0 —Permeability of the vacuum

S_z —Axial magnetic pole area

S_R —Radial magnetic pole area

δ_z —Axial air gap length

δ_R —Radial air gap length

Based on the Kirchoff's laws of the magnetic circuit ($\sum F=0$ and $\sum \phi_i=0$), the biased flux of each air gap in figure 2 can be calculated as follows:

$$\begin{cases} \phi_{z1} = [F_m (G_g - G_z) + N_R i_x (G_{x2} - G_{x1}) + N_R i_y (G_{y2} - G_{y1}) - N_z i_z (G_g - G_z + 2G_{z2})] G_{z1} / G_g \\ \phi_{z2} = [F_m (G_g - G_z) + N_R i_x (G_{x2} - G_{x1}) + N_R i_y (G_{y2} - G_{y1}) + N_z i_z (G_g - G_z + 2G_{z1})] G_{z2} / G_g \\ \phi_{x1} = [F_m (G_g - G_x - G_y) + N_z i_z (G_{z2} - G_{z1}) - N_R i_x (G_{y2} - G_{y1}) - N_R i_x (G_g - G_x + 2G_{x2})] G_{x1} / G_g \\ \phi_{x2} = [F_m (G_g - G_x - G_y) + N_z i_z (G_{z2} - G_{z1}) - N_R i_x (G_{y2} - G_{y1}) + N_R i_x (G_g - G_x + 2G_{x1})] G_{x2} / G_g \\ \phi_{y1} = [F_m (G_g - G_x - G_y) + N_z i_z (G_{z2} - G_{z1}) - N_R i_x (G_{x2} - G_{x1}) - N_R i_y (G_g - G_y + 2G_{y2})] G_{y1} / G_g \\ \phi_{y2} = [F_m (G_g - G_x - G_y) + N_z i_z (G_{z2} - G_{z1}) - N_R i_x (G_{x2} - G_{x1}) + N_R i_y (G_g - G_y + 2G_{y1})] G_{y2} / G_g \end{cases} \quad (3)$$

where $G_z = G_{z1} + G_{z2}$; $G_x = G_{x1} + G_{x2}$; $G_y = G_{y1} + G_{y2}$;

$$G_g = G_z + G_x + G_y;$$

$N_z i_z$ — Ampere-turn of axial control coils,
 $N_R i_r$ — Ampere-turn of radial control coils,
 $r = x, y$

Expression on Magnetic Attractive Force

If the rotor has small positive displacements x or y in radial direction or z in axial direction, a negative direction resulting force is needed to make the rotor go back to the balance position. The magnetic attractive force can be calculated as follow:

$$F_j = F_{j2} - F_{j1} = \frac{\phi_{j2}^2 - \phi_{j1}^2}{2\mu_0 S_j} \quad (4)$$

where $j=x, y, z$; $S_x=S_y=S_R$, S_R is radial magnetic pole area and S_z is axial magnetic pole area; μ_0 is permeability of the vacuum; F_{j2} is magnetic attractive force acted in negative j -direction of the rotor and F_{j1} is magnetic attractive force acted in positive j -direction of the rotor.

Substituting Eqs.(2) and (3) into Eq.(4), linearizing it and neglecting the dimensionless of over two rank near the balance position (x, y are much smaller than radial air gap length δ_R , z is much smaller than axial air gap length δ_z) lead to the following expression:

$$F_j \approx \frac{\partial F_j}{\partial j} \Big|_{x=y=z=0} \cdot j + \frac{\partial F_j}{\partial I_j} \Big|_{x=y=z=0} \cdot i_j = K_j \cdot j + K_{ij} \cdot i_j \quad (5)$$

$$\text{where } j=x, y, z; \begin{cases} K_z = -\frac{8\mu_0 \cdot F_m^2}{\left(\frac{2\delta_z}{S_z} + \frac{\delta_R}{S_R}\right)^2 \delta_z S_z}; \\ K_{iz} = \frac{4\mu_0 \cdot F_m \cdot N_z}{\left(\frac{2\delta_z}{S_z} + \frac{\delta_R}{S_R}\right) \delta_z}; \end{cases}$$

$$\begin{cases} K_x = K_y = K_R = -\frac{\mu_0 \cdot F_m^2}{\left(\frac{\delta_z}{S_z} + \frac{2\delta_R}{S_R}\right)^2 \delta_z^2 \delta_R^3}; \\ K_{ix} = K_{iy} = K_{iR} = \frac{2\mu_0 \cdot F_m \cdot N_R}{\left(\frac{\delta_z}{S_z} + \frac{2\delta_R}{S_R}\right) \delta_R^2 S_z}; \end{cases}; K_z \text{ is called axial}$$

force-displacement coefficient, K_{iz} is called axial force-current coefficient; K_R is called radial force-displacement coefficient, K_{iR} is called radial force-current coefficient; K_z , K_{iz} , K_R and K_{iR} are constants after the configuration of the radial-axial HMB and the balance position of the rotor is determined.

Control Scheme of the Radial-axial HMB

According to the relationship among magnetic attractive force, the displacement and the control current as described in Eq.(5). The basic control scheme of radial-axial HMB is designed as shown in figure 4.

The displacement sensors measure the real positions of the rotor in the x -direction, y -direction and z -direction, and output the minus feedback signals to linear close-loop controller (based on DSP). The controller

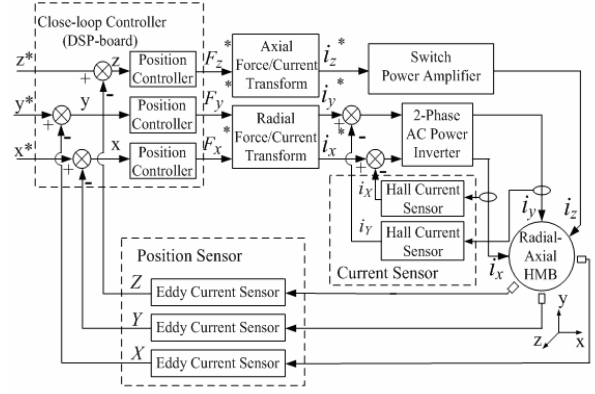


FIGURE 4: Control scheme of radial-axial HMB

compares the real positions to the position reference values set previously in the controller, and then transforms the displacement into force signals by PID controllers. The force signals are transformed into current signals to activate the power amplifier. The axial control currents provided by switch power amplifier generate controllable magnetic fluxes in the axial air gaps, so the rotor can be dragged back to the axial balance position by the suspension force generated by the resulting magnetic flux. In the radial direction, 2-phase AC control currents signals i_x^* and i_y^* are generated through force/current transformation. The hall current sensors measure the real currents in radial direction. The real currents compare with the control currents signals i_x^* and i_y^* to activate the 2-phase AC power inverter. The radial control currents provided by the 2-phase AC power inverter will generate the radial control fluxes, the suspension force will be generated by the controllable fluxes and makes the rotor suspend in the radial balance position.

PROTOTYPE PARAMETERS

The radial-axial HMB is designed to support the 5

TABLE 1: Radial-axial HMB prototype data

Item	Value	Unit
Maximum axial force $F_{z \max}$	≥ 150	N
Maximum radial force $F_{R \max}$	≥ 120	N
Air gap length δ_0	0.5	mm
Saturation induction B_s	0.8	T
Outer length	40	mm
Outer diameter	$\phi 135$	mm
Axial magnetic pole area S_z	590	mm ²
Radial magnetic pole area S_R	472	mm ²
$(N_z i_z)_{\max}$	160	At
$(N_R i_r)_{\max}$	320	At
Current density J_{\max}	4	A/mm ²
Permanent magnet material	Nd-Fe-B	

degrees of freedom magnetic suspension high speed machine tool spindle system. The design requirements and the main design parameters for the novel magnetic bearing are shown in table 1.

Parameters design demand that the axial suspension force is less than 150N and the radial suspension force is less than 120N. Due to the relationship among the air gap length, the internal MMF of the permanent magnet and the ampere turns of the control coils, the air gap length usually is 0.5~1.5mm in engineering, set $\delta_z = \delta_R = \delta_\theta = 0.5\text{mm}$ in this prototype. Usually the saturation magnetic induction B_s is set as 0.6~0.8T in engineering, as the magnetic induction of the air gap $B_g = B_s / 2$, so set $B_g = 0.4\text{T}$. The control coils adopt nominal diameter 0.67mm enamel insulated wire. The number of windings of the radial control coils and the axial control coils are 320 and 160, respectively.

3D-FEM ANALYSIS

Based on the design parameters, an experiment prototype of the novel magnetic bearing has designed in ANSOFT software. Then the prototype is simulated to analyse the magnetic circuit by using the 3-dimensional finite element method, 3D-FEM. The preprocess model of the radial-axial HMB is shown in figure 5.

The magnetic circuits are simulated and analysed by using the 3D-FEM software, and the simulated figures are given in figure 6. Figure 6(a) presents magnetic flux density distribution of permanent magnet when there is no electrical current through any of the control coils and the rotor is in the radial and axial reference balance position. As can be seen from this figure that the magnetic fluxes are symmetrical in the radial and axial direction of the radial-axial HMB, and the permanent magnetic inductions of all air gap are equal. The simulation results are coincident with the theoretic analysis of figure 2.

The magnetic induction distribution incorporated by the permanent magnetic flux and the axial control magnetic flux is shown in figure 6(b). Exciting the axial control coils, the control flux will be superimposed or subjected with the permanent magnetic flux. The figure verifies the result that the left axial air gap flux is decreased and the right axial air gap flux is increased.

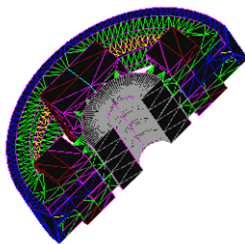
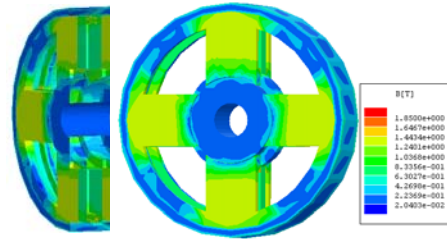
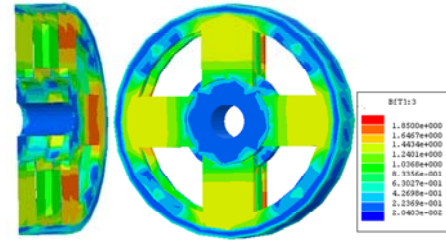


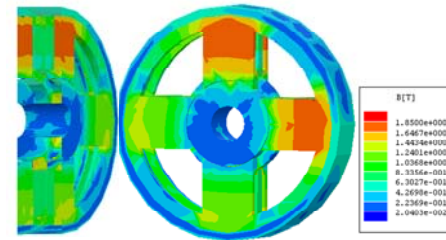
FIGURE 5: Mesh of the preprocessor model



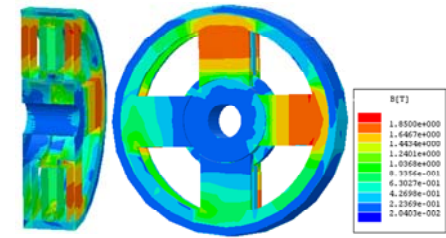
(a) Magnetic flux density distribution of permanent magnet



(b) Magnetic flux density distribution of exciting axial control coils



(c) Magnetic flux density distribution of exciting radial control coils



(d) Magnetic flux distribution of a transient working state

FIGURE 6: 3D-FEM analysis simulation of radial-axial HMB prototype

The simulation results are also coincident with the theoretic analysis of figure 2.

Figure 6(c) presents the magnetic induction distribution incorporated by the permanent magnetic flux and the radial control magnetic flux. As can be seen from the image, the radial control flux circulates only between the radial stator and the rotor, the induction value of each air gap is not equal, so the magnetic flux will be increased and the magnetic force will be increased correspondingly in the reduced air gap. In this

way, the magnetic flux will be decreased and the magnetic force will be decreased correspondingly in the increased air gap. Using the control system, the resulting force can be pointed in any direction and levitate the rotor and return to the ideal radial balance position. So the simulation results testify the feasibility that using a 2-phase AC power inverter to control the two radial degrees of freedom.

One transient working state of the prototype is simulated as shown in figure 6(e). Both the radial and the axial control coils are excited, the magnetic induction change of each air gap can be seen from the different color magnetic induction distribution nephogram. The incorporated fluxes of the radial or the axial gaps can generate the radial resulting force or the axial resulting force to overcome loads or external disturbance forces to keep the rotor in the balance position. The results of simulation have proved that the radial and the axial control flux don't influence each other.

For making the radial-axial HMB generate maximal suspension force near the balance position, maximizing the denominator of Eq.(4). That is, the radial-axial HMB generate maximal suspension force when the magnetic induction value of air gap flux increased side is maximum value B_{max} and the magnetic induction value of air gap flux decreased side is minimum value 0. According to the condition of generating maximal suspension force, using the 3D-FEM to verify the radial and the axial maximal suspension force of the radial-axial HMB. The results of the 3D-FEM analysis have shown that the axial maximal suspension force $F_{z\ max} = 167.47\text{N}$ and the radial maximal suspension force $F_{R\ max} = 134.01$. The simulation results and the above analysis present have show that the prototype is qualified with the design requirements, and some parameters have been optimized by the simulation. Moreover, the feasibility and the correctness of the theoretical methods for the configuration, magnetic path and maximum loads capacity of the radial-axial hybrid magnetic bearing are verified. This novel magnetic bearing will has a wide application in the suspending support field through further optimization design.

CONCLUSIONS

The radial-axial HMB has inner and outer two-layer control coils and two slice axial stators with radial-axial bilateral magnetic pole face structure. This design has enhanced the available area of magnetic pole, and has provided the assemble space of control coils for overcoming bigger loads or external disturbance forces. Moreover, the heat dissipation condition of the radial-axial HMB has been ameliorated. The 2 degrees of freedom in radial direction of the radial-axial HMB can

be controlled by a 2-phase AC power inverter completely. 2-phase AC power inverter is used widely in electrical drives, and the efficiency of 2-phase AC inverter is higher, the volume and cost of the power amplifier is reduced.

The radial-axial HMB is driven and controlled by AC power inverter in radial directions and DC amplifier in axial direction. So the radial control flux and the axial control flux doesn't influence each other. This conclusion is also proved by the 3D-FEM analysis. The 3D-FEM simulation results have shown that the radial control flux and the axial control flux are independent, the magnetic paths between radial direction and axial direction have no coupling. The theory analysis and simulation results have shown that the designed radial-axial HMB prototype satisfied performance requirements for a high speed machine tool spindle. The radial-axial HMB reduces the size of the overall magnetic suspension system. And it has stronger magnetic suspension force, higher efficiency and lower cost. This kind of radial-axial HMB has a potential application in all suspending fields of special support.

ACKNOWLEDGE

This work is supported by National Natural Science Foundation of China (NSFC)(50575099) and National High Technology Research and Development Program of China(863 Program)(2007AA04Z213).

REFERENCES

1. Schob R., Redemann C. and Gempp T., Radial Active Magnetic Bearing for Operational with 3-phase Power Converter, Proc. of the 4th Int. Symp. on Magnetic Suspension Technology, Gifu, Japan, pp.351-362,1997.
2. Zhu H., Yuan S., Li. B., et al, The Working Principle and Parameter Design for Permanent Magnet Biased Radial-axial Direction Magnetic Bearing, Proceedings of the CSEE, vol. 22, no. 9, pp. 54-58, September, 2002. (in Chinese)
3. Redemann C., Meuter P., Ramella A. and Gempp T., 30kW Bearingless Canned Motor Pump on the Test Bed, Proc. of the 7th Int. Symp. on Magnetic bearings, Zurich, pp.189-194, August, 2000.
4. Zhu H., Chen H., Xie Z. and Zhou Y., Configuration and Control for AC-DC Three Degrees of Freedom Hybrid Magnetic Bearings, Proc. of the 10th Int. Symp. on Magnetic bearings, Martigny, Switzerland, August, 2006.
5. Zhu H., Zhang Z., Zhu D., et al, Structure and Finite Element Analysis of an AC-DC Three Degrees of Freedom Hybrid Magnetic Bearing, Proceedings of the CSEE, vol.27, no.12, pp.77-81, April, 2007.(in Chinese).

6. Hermann P., Deutsche Patent-Offenlegungsschrift P2406790, Deutschland, pp.1-32, 1975.
7. Kim H. and Kim S., An Effective Way to Combine Radial and Axial Magnetic Bearings in a Unit, Proc. of the 10th Int. Symp. on Magnetic bearings, Martigny, Switzrland, August, 2006.
8. Liu G., Zhao L. and Jiang J., Ansoft Finite Element Analysis for Engineering Electromagnetic Field, Beijing: Press of Electronics Industry, 2005 (in Chinese).